

Review

# Solid Polymer Electrolytes for Lithium Batteries: A Tribute to Michel Armand

Alain Mauger and Christian M. Julien \* 

Institut des Minéralogie, de Physique des Matériaux et de Cosmologie, IMPMC, Sorbonne Université, UMR-CNRS 7590, 4 Place Jussieu, 75005 Paris, France; alain.mauger@sorbonne-universite.fr

\* Correspondence: christian.julien@sorbonne-universite.fr

**Abstract:** In a previous publication, a tribute to Michel Armand was provided, which highlighted his outstanding contribution to all aspects of research and development of lithium-metal and lithium-ion batteries. This area is in constant progress and rather than an overview of the work of Armand et al. since the seventies, we mainly restrict this review to his contribution to advances in solid polymer electrolytes (SPEs) and their performance in all-solid-state lithium-metal batteries in recent years.

**Keywords:** energy storage; all-solid-state lithium-metal batteries; solid polymer electrolytes; ionic conductivity

## 1. Introduction

All-solid-state lithium batteries (ASSLBs) are one of the most promising energy storage systems [1]. Their application coupling with a Li metal anode could expedite the advent of a clean energy era, especially in assembling high-energy systems [2]. Since the perceptive proposal of their application in all-solid-state lithium-metal batteries by Armand in 1978 [3], solid polymer electrolytes (SPEs) have attracted considerable attention. Along with their ease of processing, cost-effectiveness, excellent flexibility, and light weight, SPEs are inherently safer than conventional liquid electrolytes due to the absence of highly flammable carbonate solvents; thus, they offer a perfect solution to safety concerns as well as the enhancement of energy density in potential safe use with high-capacity Li-metal electrodes. Different lithium conducting groups are used in SPEs. They are presented as the foundation of macromolecular design by Meng et al. [4]. The ester group including poly(ethylene oxide) (PEO) is the most popular since the pioneering works of Armand et al., reviewed in [5]. The ester has a large dipole moment, which improves the dissociation of lithium salt and segmental motion of the polymer matrix promoting the ionic conductivity and  $\text{Li}^+$  transference number of poly(vinyl carbonate) (PVC), poly(propylene carbonate) (PPC), and poly(methyl methacrylate) (PMMA) [6]. The second group is the fluorine group, which has a strong electron-withdrawing ability, insuring a wide electrochemical stability window and high dielectric constant. The best representative of this family is poly(vinylidene fluoride) (PVDF) and the composite poly(vinylidene fluoride)-hexafluoropropylene (PVDF-HFP). These polymers can be mixed, as shown by the PEO/PVDF-based SPE used in the commercialized Bluecars of Bolloré. On another hand, the nitrile group shows poor compatibility with the lithium metal anode and will not be discussed here. Nevertheless, polymers belonging to this family, like polyacrylonitrile (PAN) can still be used in composite polymers. For instance, multilayered structures, where PAN with high electrochemical stability faces the cathode and ether or ester-based polymer contacts with the lithium anode in the multilayer SPE [7], showed remarkable performance with high-voltage cathodes [8]. The role of the architecture of the polymers will be reported for polymers of the ester or the ether families.

The chemical reaction between the polymer and the salt is of primary importance. Lithium bis(trifluoromethanesulfonyl)imide ( $\text{LiTFSI}$ ) was suggested as a conducting salt



**Citation:** Mauger, A.; Julien, C.M. Solid Polymer Electrolytes for Lithium Batteries: A Tribute to Michel Armand. *Inorganics* **2022**, *10*, 110. <https://doi.org/10.3390/inorganics10080110>

Academic Editor: Faxing Wang

Received: 2 July 2022

Accepted: 23 July 2022

Published: 29 July 2022

**Publisher's Note:** MDPI stays neutral with regard to jurisdictional claims in published maps and institutional affiliations.



**Copyright:** © 2022 by the authors. Licensee MDPI, Basel, Switzerland. This article is an open access article distributed under the terms and conditions of the Creative Commons Attribution (CC BY) license (<https://creativecommons.org/licenses/by/4.0/>).

for SPEs by Armand et al. in 1989 [9]. To date, different salts are able to become solvated in polymer matrices. Hereunder, we review recent data obtained with sulfonimide salts. To improve the mechanical strength of the SPEs, one solution is to incorporate inorganic fillers, including ceramics, nano-powders [10] or metal oxides [11], among others. Otherwise, co-polymerization is a strategy to obtain SPEs that satisfy, simultaneously, sufficient mechanical strength to prevent the formation of dendrites and good ionic conductivity. Co-polymerization and the role of the structuration of polymers will also be reported in light of the contribution of Armand et al. The understanding of the SPEs promotes not only the development of new materials and chemistry by a material genome approach [12,13], but also the key to enrich strategies for solving the issues of operating SPE-based ASSLBs, namely, higher ionic conductivity, enhanced mechanical properties and good compatibility with the electrodes.

In a previous publication, a tribute to Michel Armand was provided, which highlighted his outstanding contribution to all aspects of research and development of lithium-metal and lithium-ion batteries [5]. Herein, we report how Armand et al. contribute to the development of advanced solid polymer electrolytes and their performance in all-solid-state lithium-metal batteries in recent years.

## 2. The Lithium Sulfonimide-Based Salts

LiTFSI has been extensively used as a conducting salt for lithium metal batteries due to its advantageous stability and innocuity. TFSI<sup>−</sup> is a large highly delocalized anion, so the interactions of Li ions and the anionic structure are weakened, which insures a high number of free Li ions and a good flexibility of the polymer chains. This property of LiTFSI is due to its highly delocalized and flexible sulfonimide anion center (−SO<sub>2</sub>N<sup>(−)</sup>SO<sub>2</sub>−), which effectively reduces the interactions between TFSI<sup>−</sup> anion and Li<sup>+</sup> ion.

Widely used electrolyte salts, such as LiTFSI, generally contain the trifluoromethyl (−CF<sub>3</sub>) group, which has very low chemical and biochemical degradability. Instead, Qiao et al. proposed a trifluoromethyl-free anion, namely bis(difluoromethanesulfonyl)imide {[N(SO<sub>2</sub>CF<sub>2</sub>H)<sub>2</sub>]<sup>−</sup>, DFSI<sup>−</sup>}, as an environmentally benign and interfacially favorable anion for high-performance SPEs [14] (see Figure 1). DFSI-based salts keep the strong electron-withdrawing ability, which is essential for the dissolution and transport of ions in SPEs, and show higher chemical degradation than LiTFSI and a higher Li-only conductivity. As a result, the Li//LiFePO<sub>4</sub> cell with the LiDFSI/PEO SPE at 70 °C delivered a high capacity of 123 mAh g<sup>−1</sup> even after 140 cycles at a constant C-rate of C/3.

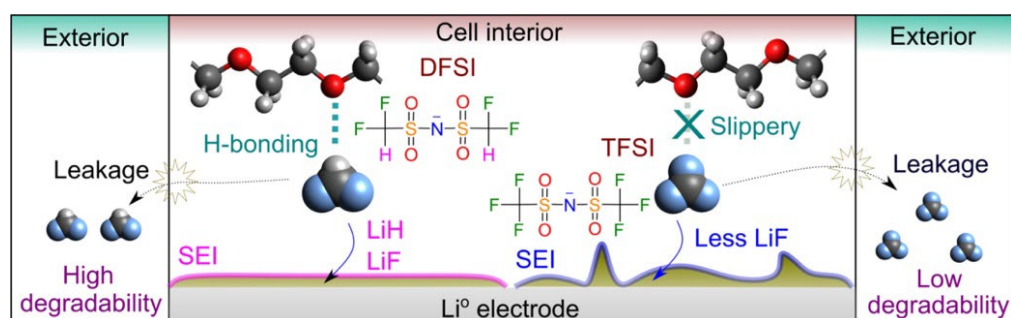


**Figure 1.** Comparison between the chemistry of CF<sub>2</sub>H- and CF<sub>3</sub>-containing compounds inside and outside a Li-metal cell. The light grey, grey, red, and light blue balls represent H, C, O, and F atoms, respectively. Reproduced with permission from Ref. [14]. Copyright 2020 Elsevier.

Another motivation to circumvent the use of LiTFSI comes from the fact that LiTFSI-based electrolytes are corrosive towards aluminum current collectors at low potentials (>3.8 V vs. Li<sup>+</sup>/Li), thereby excluding their application in 4 V-class lithium batteries. Qiao et al. solved this drawback with lithium (difluoromethanesulfonyl) (trifluoromethanesulfonyl)imide (LiDFTFSI), which remarkably suppresses the anodic dissolution of the aluminum current collector at high potentials (>4.2 V vs. Li<sup>+</sup>/Li) and improves the cycling

performance of  $\text{Li}(\text{Ni}_{1/3}\text{Mn}_{1/3}\text{Co}_{1/3})\text{O}_2$  ( $\text{NMC}_{111}$ ) cells. The replacement of LiTFSI with LiDFTFSI endows a Li// $\text{NMC}_{111}$  cell with superior cycling stability and capacity retention (87% at cycle 200) [15]. DFTFSI-based electrolytes also enable the long-life cycling of Li-S cells with high capacities and excellent Coulombic efficiencies, thus opening a new avenue toward the design of new and tailored SPEs for applications in a high-performance and safer Li-S battery, as well as other rechargeable Li batteries [16,17] (see Figure 2).

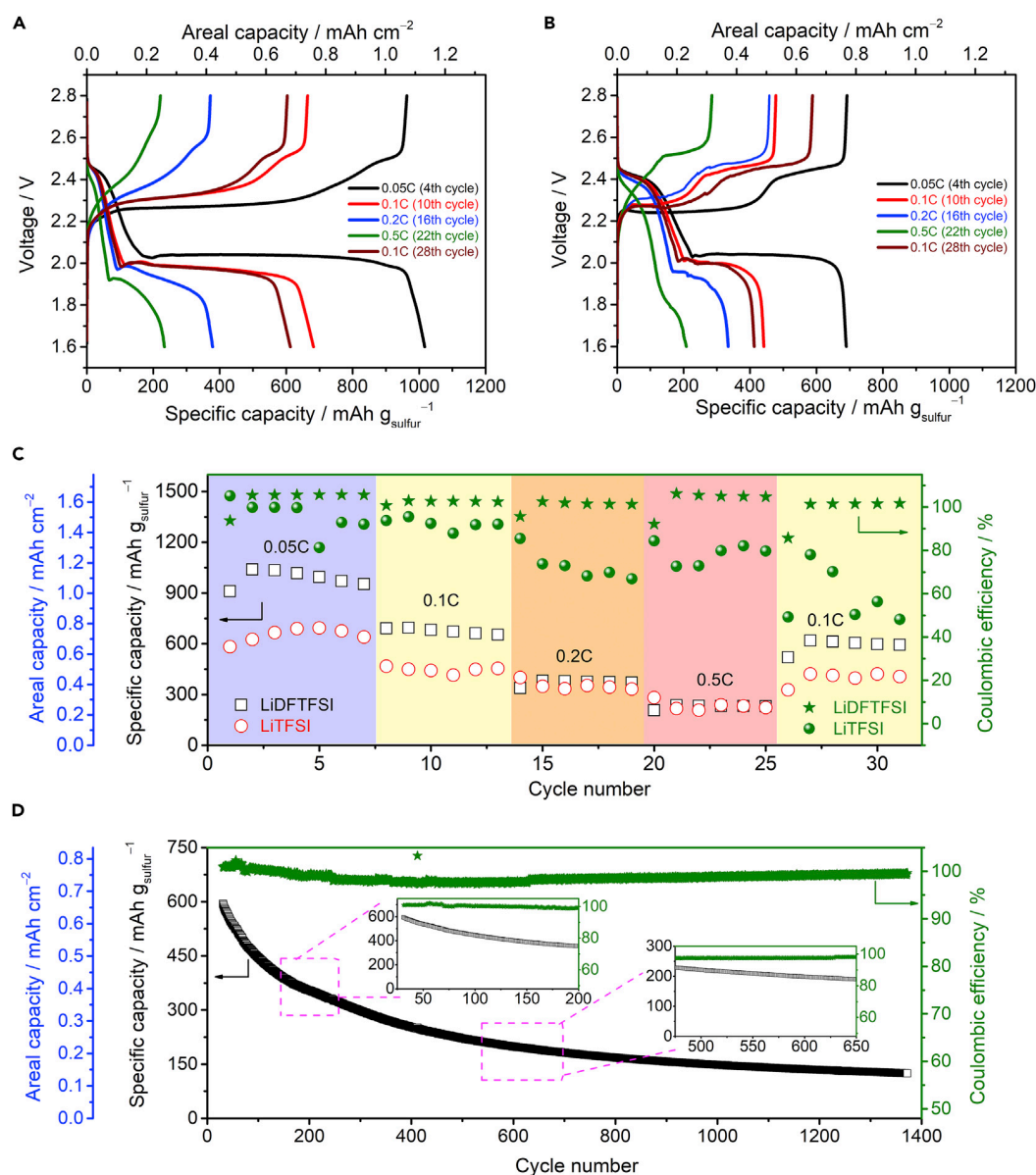


**Figure 2.** Electrochemical performance of designer anion. (A,B) Discharge/charge profiles of the Li-S cells using LiX/PEO (X = DFTFSI [A] or TFSI [B]) electrolytes at 70 °C. (C) Rate capability of the Li-S cells with LiX/PEO (X = DFTFSI or TFSI) electrolytes. (D) Long-term cycling stability of the Li-S cells using LiDFTFSI/PEO electrolytes at a discharge and charge rate of 0.1/0.1 C (after C-rate test). Reproduced with permission from Ref. [16]. Copyright 2019 Elsevier.

In the conventional PEO-LiTFSI SPE, both  $\text{Li}^+$  and the anion  $\text{TFSI}^-$  are mobile. The relative motion of anion with respect to the cation is measured by the  $\text{Li}^+$  transference number  $t_{\text{Li}^+}$ . The motion of the anion is damageable, because it generates gradient concentrations of the charges inside the SPE, which degrades the rate capability and the interfacial performance of the battery. It is thus of primary importance to immobilize the anions, i.e., to obtain a so-called single ion polymer electrolyte (SIPE) with  $\text{Li}^+$  transference number

close to unity. The co-polymerization of monomeric Li salts is a facile and efficient strategy [18,19]. In particular, high values of  $t_{\text{Li}^+} \geq 0.9$  can be obtained by replacing LiTFSI in PEO-LiTFSI by PEO-X with X = lithium propanesulfonyl(trifluoromethylsulfonyl)imide (LiPSTFSI) or X = poly[(4-styrenesulfonyl)(fluorosulfonyl)imide] (LiPSFSI). Indeed, LiPSFSI/PEO exhibited a high  $\text{Li}^+$  transference number ( $t_{\text{Li}^+} = 0.90$ ), an anodic electrochemical stability as high as 4.5 V vs.  $\text{Li}^+/\text{Li}$ , excellent interfacial compatibility with the Li-metal electrode, and its decomposition temperature was up to 200 °C [19]. This would essentially be due to the  $\text{FSO}_2^-$  group in the polyanion of LiPSFSI. A new type of single Li-ion conducting polymer electrolyte, which is prepared by simply dissolving, in PEO, the lithium salt of a super-delocalized polyanion, namely poly[(4-styrenesulfonyl)(trifluoromethyl(S-trifluoromethylsulfonylimino) sulfonyl)imide] (PSsTFSI<sup>-</sup>). The super delocalized property is due to the strong electron-withdrawing group, =NSO<sub>2</sub>CF<sub>3</sub> in  $-\text{SO}_2-\text{N}^{(-)}-\text{SO}(=\text{NSO}_2\text{CF}_3)-\text{CF}_3$ , sTFSI<sup>-</sup> [20]. It can be regarded as a derivative of TFSI<sup>-</sup> obtained by replacing a =NSO<sub>2</sub>CF<sub>3</sub> for =O group in TFSI<sup>-</sup>. The blended polymer electrolyte LiPSsTFSI/PEO exhibits a high  $\text{Li}^+$  transference number ( $t_{\text{Li}^+} = 0.91$ ) and high ionic conductivity of individual  $\text{Li}^+$  cations ( $\sigma_{\text{Li}^+} = 1.35 \times 10^{-4} \text{ S cm}^{-1}$  at 90 °C). This work was continued more recently by the insertion of LisTFSI salt in PEO by a simple casting method [21]. The PEO-LisTFSI SPE exhibits a still higher  $\text{Li}^+$  ion-only conductivity ( $\sigma_{\text{Li}^+} = 2.5 \times 10^{-4} \text{ S cm}^{-1}$  at 80 °C) owing to the better dissociation and higher mobility of  $\text{Li}^+$  ions enabled by the extremely delocalized negative charge and strong flexibility of the  $-\text{SO}_2\text{N}^{(-)}-\text{SO}(=\text{NSO}_2\text{CF}_3)-$  structure in sTFSI<sup>-</sup> with respect to TFSI<sup>-</sup>. Moreover, the interphases of Li-metal electrode|SPE formed in LisTFSI/PEO show superior stability upon storage.

Another design of anions with highly delocalized negative charges is a partial substitution of F atoms in TFSI<sup>-</sup> with H atoms, which can effectively enhance the Li-ion conductivity at a low expense of the total ionic conductivity [22]. Another strategy to overcome the low ionic conductivity and limited compatibility of LiTFSI/PEO electrolyte with lithium is the substitution of LiTFSI for lithium bis(fluorosulfonyl)imide LiFSI. LiFSI has been intensively investigated, not only in PEO [23], but also in different polymers [11,24–39] including poly-ionic liquids (PILs) [40,41], and poly(ethylene carbonate) (PEC) [42–44]. This substitution of LiFSI for LiTFSI in SPE also proved efficient in Li-S batteries [45–48]. Compared with TFSI-based SPEs, the corresponding FSI-based ones show lower glass transition temperatures ( $T_g$ ) and higher ionic conductivities, which prove the better plasticizing ability of FSI<sup>-</sup> anion vs. TFSI<sup>-</sup> anion. In addition, the formation of protective and high  $\text{Li}^+$ -conductive solid-electrolyte interphase (SEI) layers in LiFSI/PEO results in a much more stable interface resistance [23] and an improved cycle life of the Li anode [24] compared with LiTFSI/PEO. Inspired by this improved compatibility with Li anode, LiFSI was also studied as SEI-forming additive in concentration of 1–2 wt.% for SPEs [27], which effectively extended the lifespan of symmetric Li cells by forming an insulating SEI layer that prevents the continuous reduction of the SPE.

The electrochemical properties of polymer-LiFSI solid-state electrolytes are reported in the following Table 1. Some of them contain Jeffamine, of great interest for obtaining crosslinking networks in robust SPE matrices because only mild reaction conditions are required for amino groups to, respectively, react with carboxylic acid, epoxide, anhydride, etc., and the presence of EO units in Jeffamine would certainly enhance the solubility of the Li salt [49]. Further insight into the physical, chemical and electrochemical properties of FSI<sup>-</sup> can be found in [50], including its use in liquid and gel polymer electrolytes.

**Table 1.** Electrochemical performance of lithium batteries using FSI-based SPEs.  $\sigma_i$  is the conductivity at temperature mentioned in the 4th column. Current density is expressed in C-rate with equivalent in mA cm<sup>-2</sup> in parentheses.

SPE	$\sigma_i$ (S cm <sup>-1</sup> )	Cathode	T (°C)	Capacity (mAh g <sup>-1</sup> )	C-Rate	Ref.
LiFSI/PEO (EO/Li <sup>+</sup> = 20)	$3.3 \times 10^{-4}$	LFP	80	146 (1st); 144 (20th)	0.2 C (0.1)	[23]
LiFSI/PEO (EO/Li <sup>+</sup> = 20)	$8.0 \times 10^{-4}$	LFP	80	160 (1st); 144 (100th)	−0.3	[24]
LiFNFSI/PEO (EO/Li <sup>+</sup> = 20)	$5.0 \times 10^{-4}$	LFP	80	120 (570th)	0.1 C (0.1)	[11]
LiFSI/PEO + Mg <sub>3</sub> N <sub>2</sub> (EO/Li <sup>+</sup> = 20)	$1.7 \times 10^{-4}$	LFP	60	150 (10th); 125 (50th)	0.5 C (0.26)	[25]
LiFSI/PEO + N <sub>1222</sub> FSI	$2.1 \times 10^{-4}$	LFP	50	159 (1st); 152 (90th)	0.2 C (0.06)	[26]
LiTCM/PEO + LiFSI (1 wt.%)	$5.0 \times 10^{-4}$	LFP	70	117 (20th); 108 (120th)	0.3 C	[27]
LiFSI/Jeffamine (EO/Li <sup>+</sup> = 20)	$2.0 \times 10^{-4}$	LFP	50	120 (1st); 50 (1st)	0.1 C (0.1)	[28]
LiFSI/Jeffamine + PVDF (90 wt.%) (EO/Li <sup>+</sup> = 20)	$8.0 \times 10^{-4}$	LFP	70	159 (1st); 130 (1st)	0.1 C (0.1)	[29]
LiFSI/PEC (20 wt.%)	$1.6 \times 10^{-5}$	LFP	30	120 (1st)	0.05 C	[42]
LiFSI (30 wt.%) / PCL-PS (7:3 by wt)	$1.4 \times 10^{-5}$	LFP	80	131 (1st); 99 (1200th)	1 C	[30]
LiFSI/PVDF (60 wt.%) + PY <sub>12</sub> FSI (PY <sub>12</sub> <sup>+</sup> /Li <sup>+</sup> = 9:1)	$6.0 \times 10^{-5}$	LFP	25	ca 100 (1st)	2 C (0.46)	[31]
LiFSI/PVDF (60 wt.%) + PY <sub>12</sub> FSI (PY <sub>12</sub> <sup>+</sup> /Li <sup>+</sup> = 9:1)	$1.4 \times 10^{-5}$	LFP	50	130 (1st); 125 (100th)	2 C (0.46)	[32]
LiFSI/P (VDF-HFP) (16 wt.%) + N <sub>1222</sub> FSI (64 wt.%)	$8.6 \times 10^{-4}$	LFP	30	150 (1st); 140 (200th)	0.2 C (0.21)	[33]
LiFSI/P (VDF-HFP) + PGCN (10 wt.%)	$1.4 \times 10^{-4}$	LFP	26	129 (1st); 92 (400th)	0.5 C	[34]
LiFSI/P (DADMA) FSI (DADMA <sup>+</sup> /Li <sup>+</sup> = 2:3)	$0.7 \times 10^{-4}$	LFP	80	160 (5th); 160 (30th)	−0.04	[40]
LiFSI-SN/P (VDF-HFP) + ETPTA (15 wt.%)	$1.0 \times 10^{-3}$	LFP	25	130 (10th); 129 (800th)	1.0 C	[35]
LiFSI (40 wt.%) / PVDF + PAA (2 wt.%)	$1.3 \times 10^{-4}$	LCO	30	120 (1st); 80 (1000th)	−0.088	[36]
LiFSI/PVDF (60 wt.%)	$2.5 \times 10^{-4}$	LCO	25	109 (1st); 119 (200th)	−0.15	[37]
LiFSI/PEC (EC/Li <sup>+</sup> = 5:6)	$2.7 \times 10^{-5}$	LMO	60	95 (1st); 85 (10th)	−0.02	[43]
LiFSI/P (DADMA) FSI (DADMA <sup>+</sup> /Li <sup>+</sup> = 2:3)	$0.7 \times 10^{-4}$	NMC <sub>111</sub>	80	160 (5th); 130 (50th)	0.05 C (0.06)	[40]
LiFSI/TPU-HNTs (22 wt.%) + PE	$\sim 10^{-4}$	NMC <sub>811</sub>	60	103 (3rd); 102 (300th)	0.5 C	[38]
LiFSI/PVEC (16 wt.%)	$2.0 \times 10^{-4}$	NMC <sub>532</sub>	25	140 (1st); 55 (200th)	0.5 C	[39]
LiFSI (16 wt.%) / PVEC + NR (VEC/NR = 4)	$1.6 \times 10^{-4}$	NMC <sub>532</sub>	25	145 (1st); 115 (200th)	0.5 C	[39]
LiFSI/PEO (EO/Li <sup>+</sup> = 20)	$9.0 \times 10^{-4}$	Sulfur	70	420 (3rd); 550 (60th)	0.1 C (0.16)	[46]
LiFSI/PEO + LiN <sub>3</sub> (2 wt.%) (EO/Li <sup>+</sup> = 20)	$5.0 \times 10^{-4}$	Sulfur	70	850 (1st); 700 (30th)	0.1 C (0.16)	[48]
LiFSI/PEO + LICGC (3 vol.%) (EO/Li <sup>+</sup> = 20)	$8.0 \times 10^{-4}$	Sulfur	70	784 (1st)	0.1 C (0.16)	[47]

Abbreviations. LFP: LiFePO<sub>4</sub>, LCO: LiCoO<sub>2</sub>, NMC<sub>111</sub>: LiNi<sub>1/3</sub>Mn<sub>1/3</sub>Co<sub>1/3</sub>O<sub>2</sub>, NMC<sub>532</sub>: LiNi<sub>0.5</sub>Mn<sub>0.3</sub>Co<sub>0.2</sub>O<sub>2</sub>, NMC<sub>622</sub>: LiNi<sub>0.6</sub>Mn<sub>0.2</sub>Co<sub>0.2</sub>O<sub>2</sub>, NMC<sub>811</sub>: LiNi<sub>0.8</sub>Mn<sub>0.1</sub>Co<sub>0.1</sub>O<sub>2</sub>, LMO: LiMn<sub>2</sub>O<sub>4</sub>, N<sub>1222</sub>FSI: *N,N*-triethyl-*N*-methyl-ammonium bis(fluorosulfonyl)imide, LiTCM: lithium tricyanometanide, Jeffamine: polymer matrix containing polyether side moieties, HFP: hexafluoro propylene, PEC: poly (ethylene carbonate), PVDF: poly(vinylidene fluoride), PCL/PS: hyperbranched polycaprolactone/polystyrene copolymer, PY<sub>12</sub>FSI: *N*-ethyl-*N*-methylpyrrolidinium bis(fluorosulfonyl) imide, PGCN: (porous graphitic carbon nitride), SN: succinonitrile, ETPTA: (ethoxylated trimethylolpropane triacrylate), PAA: (polyacrylic acid), PEC: poly (ethylene carbonate), DADMA: diallyldimethylammonium, TPU-HNTs (thermoplastic polyurethane–halloysite nanotubes), PVEC: poly (vinyl ethylene carbonate), NR: (silica-nanoresin), LICGC<sup>TM</sup> is a lithium ion conducting glass ceramic.

Note, the SPEs in cells with cathodes of the 4-V class reported in Table 1 are not based on PEO, because PEO oxidizes at high potential, which is responsible for a poor cycle life [51]. The best that has been observed with PEO and NMC was obtained with the addition of 10 vol.% Li<sub>6.55</sub>Ga<sub>0.15</sub>La<sub>3</sub>Zr<sub>2</sub>O<sub>12</sub> (LLZO) ceramic garnet to PEO-LiFSI (EO/Li<sup>+</sup> = 20), 5 vol.% of LiOH was also added to the SPE to promote the cleavage of the S–F bond in the LiFSI salt, leading to the spontaneous formation of LiF, to obtain a less resistive and more robust SEI. The NMC<sub>622</sub>//Li metal cells at C/20 and 70 °C with this SPE delivered the capacity on 164 mAh g<sup>-1</sup>, reduced to 145 mAh g<sup>-1</sup> in the 20th cycle, while the Coulombic efficiency (CE) of the cell remained over 90% [52].

Tong et al. studied SPEs comprising lithium-fluorinated sulfonimide, including Li[(FSO<sub>2</sub>)(RFSO<sub>2</sub>)N] (R-F = n-C<sub>m</sub>F<sub>2m+1</sub>, m = 0 (LiFSI), 1 (LiFTFSI), 2 (LiFPFSI), and 4 (LiFNFSI)) and Li[(CF<sub>3</sub>SO<sub>2</sub>)(2)N] (LiTFSI), as conducting salt and poly(ethylene oxide) (PEO) as polymer matrix (Figure 3) [24]. The cycling stabilities for both the Li//Li and Li//LiFePO<sub>4</sub> cells with Li[(FSO<sub>2</sub>)(RFSO<sub>2</sub>)N] systematically outperform those with LiTFSI at 0.2 mA cm<sup>-2</sup> at 80 °C (i.e., being increased in the order of LiTFSI < LiFTFSI, LiFPFSI < LiFSI < LiFNFSI for Li//Li cells, and in the order of LiTFSI < LiFSI, LiFTFSI < LiFPFSI < LiFNFSI for Li//LiFePO<sub>4</sub> cells). Therefore, even though LiFPFSI/PEO polymer electrolyte possesses a high ionic conductivity of 6.2 × 10<sup>-4</sup> S·cm<sup>-1</sup> at 80 °C, which qualifies LiFPFSI as a potential salt for SPEs-based Li batteries [53], LiFNFSI is preferred. The Li/PEO-LiFNFSI/LiFePO<sub>4</sub> cell demonstrated 80.8% capacity retention after 570 cycles at 1.0 °C and 80 °C.

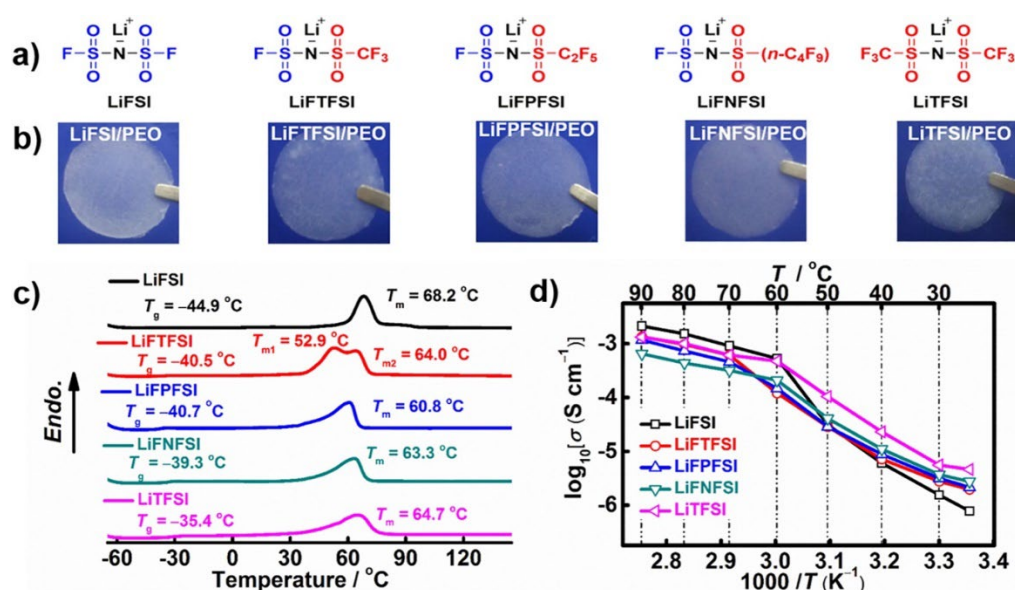


**Figure 3.** Chemical structures of LiX (a), and photographs (b), phase behaviors (c), and ionic conductivities ( $\sigma$ ) (d) of solid polymer electrolytes of LiX/PEO (X = FSI, FTFSI, FPFSI, FNFSI, and TFSI; [EO]/[Li<sup>+</sup>] = 20, by mol). Reproduced with permission from Ref. [24]. Copyright 2020 Elsevier.

Recently, a new kind of sulfonimide salt, namely, Li(trifluoromethanesulfonyl)(*N*-ethyl-*N*-methyl-sulfamoyl)imide (LiTFEMSI) was proposed by Martinez-Ibanez et al. [54]. The effective reduction in anion mobility allowed the obtention of PEO/LiTFEMSI SPE with a Li-ion conductivity as high as  $2.2 \times 10^{-4} \text{ S cm}^{-1}$  at  $70^\circ\text{C}$  and  $t_{\text{Li}^+} = 0.64$ . Moreover, the excellent electrochemical stability against oxidation up to 4.6 V vs. Li<sup>+</sup>/Li and the avoidance of Al current collector corrosion evidence the potential application of LiTFEMSI salt for >4 V-class batteries.

### 3. Polymer Architecture

#### 3.1. Copolymerization

Copolymerization allows the combination of different functional groups to obtain SPEs with optimized properties by the synergetic effects of the different groups. Oligomer polyethylene glycol (PEG) with ether groups is often used as the ionic conducting segment, in particular those with allylic end groups. As an example, Bouchet et al. synthesized a multifunctional single-ion polymer electrolyte based on polyanionic block copolymers comprising polystyrene segments. It overcomes most of the above limitations, with a Li<sup>+</sup> transference number close to unity, excellent mechanical properties and an electrochemical stability window spanning 5 V vs. Li<sup>+</sup>/Li [55].

Another attempt to increase the conductivity is to use co-doping with a more conductive polymer, in particular aliphatic carbonates to take advantage of the coordination between Li<sup>+</sup> and a carbonyl group resulting in moderate ionic conductivity and a high Li<sup>+</sup> transference number [56]. Meabe et al. synthesized poly(ethylene oxide) segments linked by carbonate groups with cross-linkable methacrylic pendant groups. Once the polymer and LiTFSI were mixed, the poly(ethylene oxide carbonate) was cross-linked by UV light producing a free standing SPE [57]. For the optimized salt concentration (30 wt.% LiTFSI equivalent to an O:Li mole ratio of 1:16), the conductivity reached  $1.3 \times 10^{-3} \text{ S cm}^{-1}$  and the Li<sup>+</sup> transference number was 0.59. The corresponding Li//Li cell at  $70^\circ\text{C}$ , showed low overpotential values and a stable solid-electrolyte interphase layer. PEO-poly(propylene carbonate) (PPC) composite polymer does not work with LiTFSI, because of the interdiffusion between LiTFSI and the two polymers. Arrese-Igor et al. unveiled the Li salt interdiffusion occurring between the two different dual-ion conducting polymer electrolytes: the replacement of LiTFSI by lithium poly[(4-styrenesulfonyl) (trifluoromethanesulfonyl)imide] (LiPSTFSI), with the anionic moiety  $\text{SO}_2\text{N}^-(\text{SO}_2\text{CF}_3)$  immobilized, hinders such unwanted

interdiffusion [58] (see Figure 4). In addition, the use of two different polymers (PEO and PPC), one for the cathode and another one as electrolyte was used for chemical stability allowing compatibility with the positive electrode and lithium metal anode.

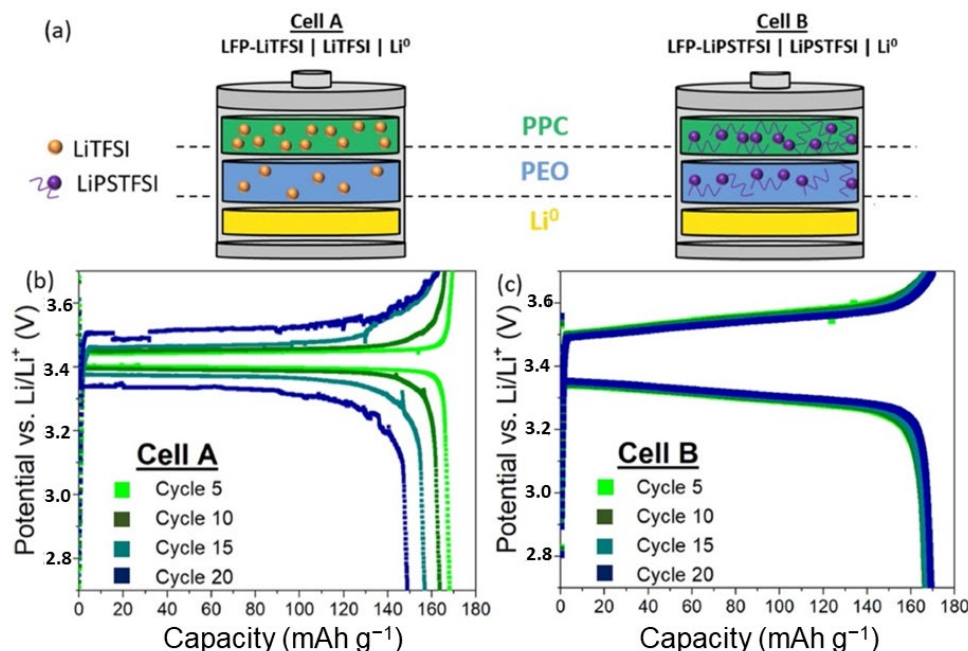


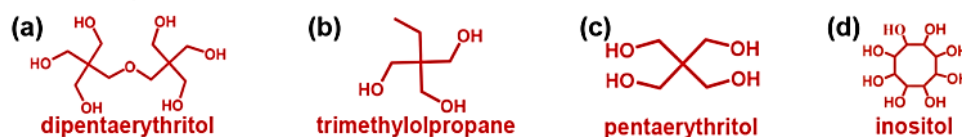
**Figure 4.** Proof-of-concept full cells of dual-layer polymer electrodes. Galvanostatic cycling of cells including different polymer-salt configurations described in (a). Schematics show Li conducting complexes LiTFSI (orange) and LiPSTFSI (purple), SPE PEO (blue), and catholyte PPC (green). Voltage profile upon cycling for the initial cycles at C/20 of (b) Cell A and (c) Cell B. Reproduced with permission from Ref. [58]. Copyright 2022 Elsevier.

The  $\text{LiFePO}_4//\text{Li}$  cells with LiPSTFSI, PPC as catholyte, and PEO as solid-electrolyte separator, display an outstanding cycling performance, with above 80% capacity retention at C/10, over 120 cycles, nearly reaching the theoretical capacity of  $170 \text{ mAh g}^{-1}$ , and maintaining 99% Coulombic efficiency. Moreover, PPC has a high electrochemical stability up to 4.6 V, so that its use as catholyte allows for the use of the SPE with a cathode of the 4 V-family, even with PEO as the electrolyte. The same double-layer SPE integrated in a cell with  $\text{LiNi}_{0.6}\text{Mn}_{0.2}\text{Co}_{0.2}\text{O}_2$  ( $\text{NMC}_{622}$ ) and Li-metal electrodes employing a high-areal-capacity electrode ( $1 \text{ mAh cm}^{-2}$ ) cycled between 2.7 and 4.2 V vs.  $\text{Li}^+/\text{Li}$  at C/20 and  $70^\circ\text{C}$  delivered an initial capacity of  $160 \text{ mAh g}^{-1}$ , maintained at  $130 \text{ mAh g}^{-1}$  after 80 cycles [59]. These results demonstrate the high-energy promise of the dual-layer polymer electrolyte concept to the next generation of all-solid-state lithium batteries. They also evidence the promise of the LiPSTFSI salt, since the grafting of TFSI<sup>-</sup> to the polystyrene chain effectively minimizes its mobility, which increases the  $\text{Li}^+$  transference number of this double-layer polymer SPE to 0.98. The SEI formed between the Li-metal anode and LiPSTFSI/PEO tends to be very resistive. To overcome this drawback, Martinez-Ibanez et al. introduced LiFSI as a dopant level (2 wt.%) into the LiPSTFSI/PEO to obtain an SPE; this type of electrolyte is also known as additive-containing single Li-ion conductor (ACSLIC) [60]. This choice was motivated by the fact that the reduction of FSI<sup>-</sup> on the surface of the Li electrode leads to the rapid formation of a stable LiF-rich SEI layer. Moreover, this dopant promoted the interaction between LiPSTFSI and PEO. As a result, the  $\text{Li}^+$  transference number of the ACSLIC was raised to 0.63. The 2 wt.% LiFSI-additive increased the ionic conductivity by one order of magnitude.

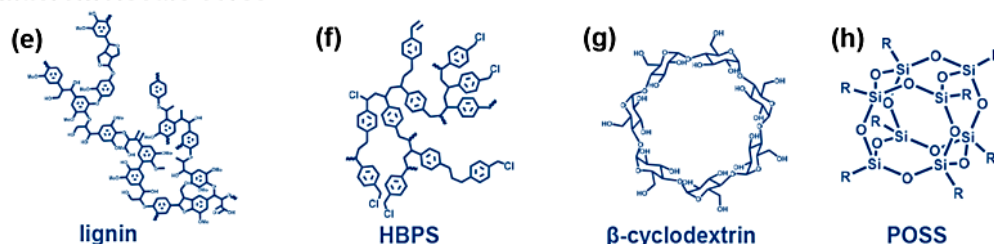
### 3.2. Branched Architecture

Compared with linear polymers, branched architectures effectively increase polymer segmental mobility, restrain crystallization, and reduce chain entanglement, which increases Li transport [61]. Branched polymers include starlike polymers (SPs), comb-like polymers (CPs), bottlebrush-like polymers (BBPs), and hyperbranched polymers (HBPs) (see Figure 5 for chemical structures).

#### Small compound cores



#### Macromolecule cores



#### Crosslinked cores

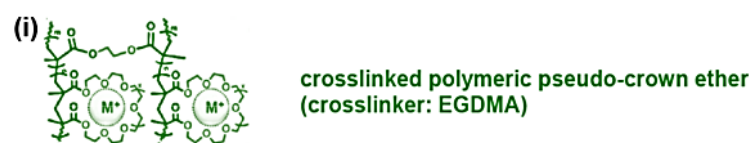


**Figure 5.** Chemical structures of (a–d) small compounds, (e–h) macromolecules, and (i) cross-linked cores for SP-PEs. (i) Reproduced with permission from Ref. [61]. Copyright 2021 ACS.

Comb-like polymers are a variety of branched polymers where monomers, oligomers, or macromonomers are anchored onto polymeric backbones with the aid of various chemical junctions. These backbones have a linear structure, and the grafted molecular chains, referred to as side chains, dangle along the backbone [62]. They are one of the most auspicious candidates for building fully amorphous and highly conductive SPEs [49,63]. Wang et al. synthesized two kinds of comb-like polymers, containing either polymethacrylate or polyacrylate as main chains, which were comparatively investigated, aiming to illustrate the role of polymer backbones. They found that the polymethacrylate-based SPEs show significantly improved interfacial stability against lithium metal electrode compared with the polyacrylate-based ones, due to the elimination of an electrochemically labile C–H moiety at the alpha position of the carbonyl group (C=O) in the polyacrylate structure [64]. This result illustrates the key role played by the structure of the polymer main backbone in determining the properties of SPEs. It also proposes a new family of SPEs, consisting of lithium bis(fluorosulfonyl)imide (LiFSI) and poly(methoxy-polyethylene glycol methacrylate) (i.e., LiFSI/P(CH<sub>3</sub>-MPEGMA)), with high ionic conductivities at room temperature, but also insights into developing a lithium-metal-friendly SPE for safe lithium metal batteries, with a conductivity of  $3.69 \times 10^{-5} \text{ S cm}^{-1}$  and stable galvanostatic cycling of the Li symmetric cells over more than 1500 h at 80 °C with a current density of  $0.2 \text{ mA cm}^{-2}$  and a half-cycle duration of 2 h (see Figure 6).

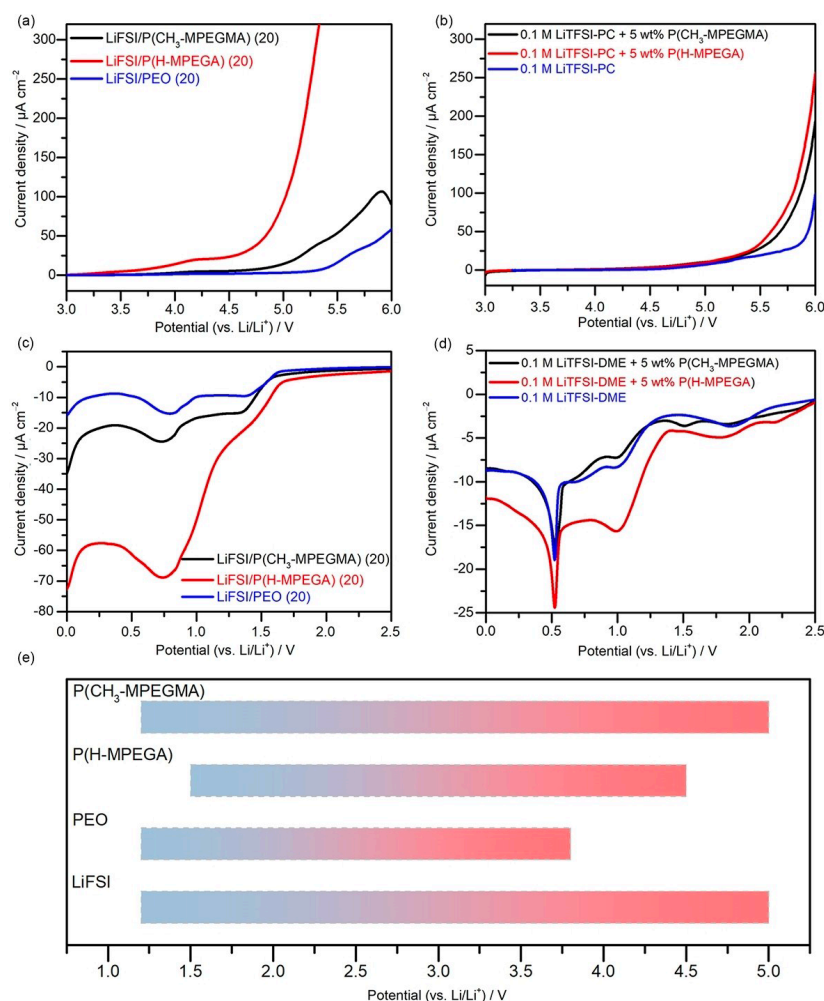


**Figure 6.** Electrochemical properties of the comb-like SPEs. (a) Linear sweep voltammograms (LSV) measured on stainless electrode for LiFSI/poly(methoxy-polyethylene glycol methacrylate) (P(CH<sub>3</sub>-MPEGMA)), LiFSI/poly(methoxy-poly-ethylene glycol acrylate) (P(H-MPEGA)), and LiFSI/PEO at a fixed salt concentration of [EO]/[Li<sup>+</sup>] = 20 (temperature: 80 °C; scan rate: 0.5 mV s<sup>-1</sup>). (b) LSV profiles measured on Pt electrode for the liquid electrolytes of 0.1 mol L<sup>-1</sup> LiTFSI-PC with or without addition of comb-like polymers (temperature: 25 °C; scan rate: 0.5 mV s<sup>-1</sup>). (c) LSV profiles measured on stainless electrode for the three SPEs (temperature: 80 °C; scan rate of 0.5 mV s<sup>-1</sup>). (d) LSV profiles measured on Ni electrode for the liquid electrolytes of 0.1 mol L<sup>-1</sup> LiTFSI-DME with or without addition of comb-like polymers. (e) Schematic electrochemical stability diagram of the comb-like polymers and other related electrolyte components. Reproduced with permission from Ref. [64]. Copyright 2022 Wiley.

In Table 1, one result is reported with long-subchain-hyperbranched copolymers from various compositions of AB<sub>2</sub> macromonomers of PCL-2N<sub>3</sub> (polycaprolactone, PCL) and PS-2N<sub>3</sub> (polystyrene) doped with LiFSI [30]. The good electrochemical performance of the Li//LiFePO<sub>4</sub> cell reported in Table 1 is due to the synergetic effect of the architecture of the polymer, the co-polymerization and the choice of the LiFSI salt. First, the hyperbranched architecture effectively suppressed the crystallization of PCL, leading to a purely amorphous state, which is beneficial for ionic conductivity. Also, at the same molecular weight, branched polymers (BPs) have shorter chains than linear analogues, which can reduce chain entanglement and the viscosity of the polymer. Second, polystyrene enhances the mechanical strength of the SPE, which is needed to avoid the growth of dendrites on the Li anode. Third, we have already discussed the advantage of the LiFSI salt. As a result, this SPE exhibited high ionic conductivity ( $1.59 \times 10^{-4}$  S cm<sup>-1</sup> at 80 °C), a broad

electrochemical stability window ( $>4.6$  V) and a high  $\text{Li}^+$  transference number ( $>0.40$ ). Block polymerization is another strategy to build composite polymers, since it permits modification of the architecture of the polymers at the molecular level [28,55].

#### 4. Design of the Cathode

While efforts have been focused on the electrolytes to avoid the formation of dendrites on the Li anode, much less attention is paid to the design of high-performance positive electrodes. However, their design is crucial to improve the electrochemical performance of the Li-metal batteries (LMBs) [65]. Most of the intercalation cathodes utilized for rechargeable LMBs are directly inherited from lithium-ion battery technology. However, the properties for Li metal are distinct from those of the graphitic anode utilized in lithium-ion batteries (LIBs). In particular, the degree of volume expansion and contraction during cycling is significantly higher for the lithium metal anode. Also, lithium metal is more chemically reactive compared to a graphite anode, which may impact the properties of the cathode via cathode–anode cross-talk. Therefore, the replacement of the graphite anode by a lithium metal anode requires rational design of the intercalation cathode, particularly the electro-inactive materials including catholyte and binding polymers [66]. PVDF and its derivatives have been among the most commonly used binder materials. However, PVDF has a very low ionic conductivity. Also, it requires the use of the toxic organic solvent, *N*-methyl-2-pyrrolidone (NMP). Therefore, different attempts are being made to replace it with more conductive and environmentally friendly polymeric materials [67,68]. In recent years, several kinds of alternative polymeric material have been investigated for high-voltage cathodes [69–71], such as lithium poly(acrylic acid) (LiPAA) [72], and PAA-based amphiphilic bottlebrush polymers [73]. Santiago et al. proposed a new strategy [74]. They reported a new single lithium-ion-conducting (SLIC) polysalt based on imide ring and  $(\text{TFSI}^-)$  anion as dual-functional materials for 4-V-class rechargeable LMBs. The polysalt itself could act as a binding agent for gluing active materials and conductive carbon, and could transport  $\text{Li}^+$  ions within the cathode materials due to its ionic nature; thus, the polysalt is named as Binderlyte (i.e., binder + catholyte). The implementation of designer Binderlyte endows the  $\text{Li}/\text{Li}(\text{Ni}_{1/3}\text{Mn}_{1/3}\text{Co}_{1/3})\text{O}_2$  (NMC<sub>111</sub>) with superior cycling stability and capacity retention even at an extremely high C-rate of 10 C. Another advantage of Binderlyte concerns the so-called calendaring (the continuous roll compaction that is the established method for industrial scale). As electrodes are compressed, thermal and electrical conductivity are improved, but high compression rates can lead to high mechanical levels of stress on active material particles which is detrimental to cell performance and lifetime [75]. The soft and flexible nature of Binderlyte allows the thick NMC cathode to operate at extremely low porosity (20 vol.%) with almost no capacity decay. Binderlyte is thus proven as a successful strategy and should encourage further works on the development of a new generation of binder materials.

#### 5. Conclusions and Perspectives

Owing to progress in the recent years, some SPEs can now exhibit room temperature ionic conductivity of  $\sim 10^{-4}$  S  $\text{cm}^{-1}$ , with oxidative stability approaching 5 V. With functional fillers, composite SPEs can even have conductivity up to  $10^{-3}$  S  $\text{cm}^{-1}$ . The efforts to synthesize single-ion SPEs has been successful, and some of them have  $t_{\text{Li}^+}$  close to unity, which promotes uniform transport of  $\text{Li}^+$ , while high shear modulus can be obtained by appropriate polymer architectures. The use of soft polymers on the lithium anode site can improve the contact between the anode and the SPE.

Polymers are crucial components of the cathode. Polymer binders insure the homogeneity of active material distribution and adhesion between nanoparticles of the active material. Some of these are now proposed to eliminate the use of toxic NMP in cathode slurry preparation.

When a conventional organic carbonate electrolyte is used in an LMB, a passivation layer forms between the anode and the electrolyte during cycling. However, this passivation

layer shows poor flexibility, which makes it vulnerable to volume changes on the lithium anode interface. Polymer artificial solid-electrolyte interphases were developed to improve interfacial stability. Another solution is the use of a second polymer, such as PSTFSI, to improve interfacial stability. This is a promising solution needing further investigation to obtain an SPE-Li metal interface with high ionic conductivity and a high  $\text{Li}^+$  transference number to promote uniform transport of  $\text{Li}^+$ .

Despite these advances in the design of polymers, interlayers and electrodes, further challenges should be addressed. The ionic conductivity of the SPEs is still one or two orders of magnitude smaller than that of liquid electrolytes. To overcome this drawback, efforts are being made to reduce the thickness of the SPE. However, the change in volume inside the cell upon cycling will result in the formation of holes in the membrane if it is too thin. Therefore, efforts are still needed to control the thickness during manufacturing and to design thin polymer membranes without sacrificing their mechanical strength. Finally, the huge need for high-performing lithium secondary rechargeable batteries has boosted the research on SPEs, which has resulted in considerable progress in the development of polymer materials for high-energy-density Li-metal polymer (LMP) batteries. They are now a promising solution that could participate in the breakthrough in energy storage that is needed in the fight against global warming and the abandonment of fossil fuels.

It is remarkable to note that the research of Professor Armand is currently applied in real electric transport industries. The solid-state LMP battery technology developed by Blue Solutions, a unit of the Bolloré Group, is now used to power different models of electric transit buses. Thanks to the intelligent interplay of innovative charging and battery technology, the multiplexing of the communication systems and finally its avant-garde design, this technology brings a whole new dimension to electromobility. The fleet of electric buses of the public transport operator RATP, in Paris (France), is equipped with Bluebus 5SE model. These Bolloré 12-metre (39-foot) electric buses emblazoned with the words “100 percent electric vehicle” are fitted with a new generation of “high energy density and optimal safety” batteries spread around the roof and rear of the vehicle. Bluebus’s six-meter minibus, which is leased through the Bluestation turnkey service, is designed for historical city centers, and can accommodate up to 22 passengers. It is equipped with three solid-state LMP batteries, which deliver a range of up to 180 km. Bluebus has sold over 280 units of its six-meter minibus, which is now in operation in more than 60 towns and cities throughout France. Bolloré’s technology is also used by Daimler in its eCitaro electric transit bus. As standard, the roof batteries of the eCitaro are supplemented by four additional batteries at the rear. Each nickel-manganese-cobalt (NMC) type battery consists of a control unit and 15 cell modules, each with 12 cells, for a total capacity of 243 kWh. The standard eCitaro has a range of up to 200 km.

**Author Contributions:** Writing—original draft preparation, A.M.; writing—review and editing, C.M.J. All authors have read and agreed to the published version of the manuscript.

**Funding:** This research received no external funding.

**Institutional Review Board Statement:** Not applicable.

**Informed Consent Statement:** Not applicable.

**Data Availability Statement:** Not applicable.

**Conflicts of Interest:** The authors declare no conflict of interest.

## References

1. Chen, Y.; Wen, K.; Chen, T.; Zhang, X.; Armand, M.; Chen, S. Recent progress in all-solid-state lithium batteries: The emerging strategies for advanced electrolytes and their interfaces. *Energy Storage Mater.* **2020**, *31*, 401–433. [[CrossRef](#)]
2. Judez, X.; Eshetu, G.G.; Li, C.; Rodriguez-Martinez, L.M.; Zhang, H.; Armand, M. Opportunities for rechargeable solid-state batteries based on Li-intercalation cathodes. *Joule* **2018**, *2*, 2208–2224. [[CrossRef](#)]
3. Armand, M.; Chabagno, J.M.; Duclot, M.J. Polymeric solid electrolytes. In Proceedings of the Extended Abstracts of the 2nd International Conference on Solid Electrolytes, St. Andrews, UK, 20–22 September 1978.

4. Meng, N.; Lian, F.; Cui, G.L. Macromolecular design of lithium conductive polymer as electrolyte for solid-state lithium batteries. *Small* **2021**, *17*, 2005762. [[CrossRef](#)]
5. Mauger, A.; Julien, C.M.; Goodenough, J.B.; Zaghbi, K. Tribute to Michel Armand: From rocking chair—Li-ion to solid-state lithium batteries. *J. Electrochem. Soc.* **2020**, *167*, 070507. [[CrossRef](#)]
6. Zhang, J.J.; Yang, J.F.; Dong, T.T.; Zhang, M.; Chai, J.C.; Dong, S.M.; Wu, T.Y.; Zhou, X.H.; Cui, G.L. Aliphatic polycarbonate-based solid-state polymer electrolytes for advanced lithium batteries: Advances and perspective. *Small* **2018**, *14*, 1800821. [[CrossRef](#)] [[PubMed](#)]
7. Liang, J.Y.; Zeng, X.X.; Zhang, X.D.; Zuo, T.T.; Yan, M.; Yin, Y.X.; Shi, J.L.; Wu, X.W.; Guo, Y.G.; Wan, L.J. Engineering Janus interfaces of ceramic electrolyte via distinct functional polymers for stable high-voltage Li-metal batteries. *J. Am. Chem. Soc.* **2019**, *141*, 9165–9169. [[CrossRef](#)]
8. Duan, H.; Fan, M.; Chen, W.P.; Li, J.Y.; Wang, P.F.; Wang, W.P.; Shi, J.L.; Yin, Y.X.; Wan, L.J.; Guo, Y.G. Extended electrochemical window of solid electrolytes via heterogeneous multilayered structure for high-voltage lithium metal batteries. *Adv. Mater.* **2019**, *31*, 1807789. [[CrossRef](#)]
9. Armand, M.; Gorecki, W.; Andreani, R. *Second International Meeting on Polymer Electrolytes*; Scrosati, B., Ed.; Elsevier: London, UK, 1990; p. 91.
10. Syzdek, J.; Armand, M.; Marcinek, M.; Zalewska, A.; Zukowska, G.; Wiczonek, G. Detailed studies on the fillers modification and their influence on composite, poly(oxethylene)-based polymeric electrolytes. *Electrochim. Acta* **2010**, *55*, 1314–1322. [[CrossRef](#)]
11. Judez, X.; Piszcz, M.; Coia, E.; Li, C.; Aldalur, I.; Oteo, U.; Zhang, Y.; Zhang, W.; Rodriguez-Martinez, L.M.; Zhang, H.; et al. Stable cycling of lithium metal electrode in nanocomposite solid polymer electrolytes with lithium bis (fluorosulfonyl)imide. *Solid State Ion.* **2018**, *318*, 95–101. [[CrossRef](#)]
12. Mauger, A.; Armand, M.; Julien, C.M.; Zaghbi, K. Challenges and issues facing lithium metal for solid-state rechargeable batteries. *J. Power Sources* **2017**, *353*, 333–342. [[CrossRef](#)]
13. Li, Y.; Li, Y.; Cui, Y. Cryogenic-electron microscopy is rapidly transforming battery research. Now, this powerful technique has been used to identify lithium hydride as a surprising culprit behind Li-ion battery failure. *Nat. Energy* **2018**, *3*, 1023–1024. [[CrossRef](#)]
14. Qiao, L.; Oteo, U.; Zhang, Y.; Pena, S.R.; Martinez-Ibanez, M.; Santiago, A.; Cid, R.; Meabe, L.; Manzano, H.; Carrasco, J.; et al. Trifluoromethyl-free anion for highly stable lithium metal polymer batteries. *Energy Storage Mater.* **2020**, *32*, 225–233. [[CrossRef](#)]
15. Qiao, L.; Oteo, U.; Matinez-Ibanez, M.; Santiago, A.; Cid, R.; Sanchez-Diez, E.; Lobato, E.; Meabe, L.; Armand, M.; Zhang, H. Stable non-corrosive sulfonimide salt for 4-V-class lithium metal batteries. *Nat. Mater.* **2022**, *21*, 455–462. [[CrossRef](#)] [[PubMed](#)]
16. Zhang, U.; Oteo, X.; Judez, J.; Eshetu, G.G.; Martinez-Ibanez, M.; Carrasco, J.; Li, C.; Armand, M. Designer anion enabling solid-state lithium-sulfur batteries. *Joule* **2019**, *3*, 1689–1702. [[CrossRef](#)]
17. Zhang, H.; Chen, F.; Lakuntza, O.; Oteo, U.; Qiao, L.; Martinez Ibanez, M.; Zhu, H.; Carrasco, J.; Forsyth, M.; Armand, M. Suppressed Mobility of Negative Charges in Polymer Electrolytes with an Ether-Functionalized Anion. *Angew. Chem. Int. Ed.* **2019**, *58*, 12070–12075. [[CrossRef](#)]
18. Ma, Q.; Xia, Y.; Feng, W.; Nie, J.; Hu, Y.-S.; Li, H.; Huang, X.; Chen, L.; Armand, M.; Zhou, Z. Impact of the functional group in the polyanion of single lithium-ion conducting polymer electrolytes on the stability of lithium metal electrodes. *RSC Adv.* **2016**, *6*, 32454–32461. [[CrossRef](#)]
19. Devaux, D.; Liénafe, L.; Beaudoin, E.; Maria, S.; Phan, T.N.T.; Gimes, D.; Giroud, E.; Davidson, P.; Bouchet, R. Comparison of single-ion-conductor block-copolymer electrolytes with polystyrene-TFSI and polymethacrylate-TFSI structural blocks. *Electrochim. Acta* **2018**, *269*, 250–261. [[CrossRef](#)]
20. Ma, Q.; Zhang, H.; Zhou, C.; Zheng, L.; Cheng, P.; Nie, J.; Feng, W.; Hu, Y.S.; Li, H.; Huang, X.; et al. Single lithium-ion conducting polymer electrolytes based on a super-delocalized polyanion. *Angew. Chem. Int. Ed.* **2016**, *55*, 2521–2525. [[CrossRef](#)]
21. Zhang, H.; Song, Z.; Yuan, W.; Feng, W.; Nie, J.; Armand, M.; Huang, X.; Zhou, Z. Impact of negative charge delocalization on the properties of solid polymer electrolytes. *ChemElectroChem* **2021**, *8*, 1322–1328. [[CrossRef](#)]
22. Zhang, H.; Oteo, U.; Zhu, H.; Judez, X.; Martinez-Ibanez, M.; Aldalur, I.; Sanchez-Diez, E.; Li, C.; Carrasco, J.; Forsyth, M.; et al. Enhanced lithium-ion conductivity of polymer electrolytes by selective introduction of hydrogen into the anion. *Angew. Chem. Int. Ed.* **2019**, *58*, 7829–7834. [[CrossRef](#)]
23. Zhang, H.; Liu, C.; Zheng, L.; Xu, F.; Feng, W.; Li, H.; Huang, X.; Armand, M.; Nie, J.; Zhou, Z. Lithium bis(fluorosulfonyl)imide/poly(ethylene oxide) polymer electrolyte. *Electrochim. Acta* **2014**, *133*, 529–538. [[CrossRef](#)]
24. Tong, B.; Wang, P.; Ma, Q.; Wan, H.; Zhang, H.; Huang, X.; Armand, M.; Feng, W.; Nie, J.; Zhou, Z. Lithium fluorinated sulfonimide-based solid polymer electrolytes for Li||LiFePO<sub>4</sub> cell: The impact of anionic structure. *Solid State Ion.* **2020**, *358*, 115519. [[CrossRef](#)]
25. Yan, M.; Liang, J.Y.; Zuo, T.T.; Yin, Y.X.; Xin, S.; Tan, S.J.; Guo, Y.G.; Wan, L.J. Stabilizing polymer-lithium interface in a rechargeable solid battery. *Adv. Funct. Mater.* **2019**, *30*, 1908047. [[CrossRef](#)]
26. Wang, W.; Fang, Z.; Zhao, M.; Peng, Y.; Zhang, J.; Guan, S. Solid polymer electrolytes based on the composite of PEO-LiFSI and organic ionic plastic crystal. *Chem. Phys. Lett.* **2020**, *747*, 137335. [[CrossRef](#)]
27. Santiago, A.; Judez, X.; Castillo, J.; Garbayo, I.; Saenz de Buruaga, A.; Qiao, L.; Baraldi, G.; Coca-Clemente, J.A.; Armand, M.; Li, C.; et al. Improvement of lithium metal polymer batteries through a small dose of fluorinated salt. *J. Phys. Chem. Lett.* **2020**, *11*, 6133–6138. [[CrossRef](#)]

28. Aldalur, I.; Martínez-Ibañez, M.; Piszcz, M.; Rodríguez-Martínez, L.M.; Zhang, H.; Armand, M. Lowering the operational temperature of all-solid-state lithium polymer cell with highly conductive and interfacially robust solid polymer electrolytes. *J. Power Sources* **2018**, *383*, 144–149. [[CrossRef](#)]
29. Aldalur, I.; Wang, X.; Santiago, A.; Goujon, N.; Echeverría, M.; Martínez-Ibañez, M.; Piszcz, M.; Howlett, P.C.; Forsyth, M.; Armand, M.; et al. Nanofiber-reinforced polymer electrolytes toward room temperature solid-state lithium batteries. *J. Power Sources* **2020**, *448*, 227424. [[CrossRef](#)]
30. Ye, W.; Zaheer, M.; Li, L.; Wang, J.; Xu, H.; Wang, C.; Deng, Y. Hyperbranched PCL/PS copolymer-based solid polymer electrolytes enable long cycle life of lithium metal batteries. *J. Electrochem. Soc.* **2020**, *167*, 110532. [[CrossRef](#)]
31. Wang, X.; Zhu, H.; Greene, G.W.; Zhou, Y.; Yoshizawa-Fujita, M.; Miyachi, Y.; Armand, M.; Forsyth, M.; Pringle, J.M.; Howlett, P.C. Organic ionic plastic crystal-based composite electrolyte with surface enhanced ion transport and its use in all-solid-state lithium batteries. *Adv. Mater. Technol.* **2017**, *2*, 1700046. [[CrossRef](#)]
32. Nti, F.; Porcarelli, L.; Greene, G.W.; Zhu, H.; Makhlooghiyazad, F.; Mecerreyes, D.; Howlett, P.C.; Forsyth, M.; Wang, X. The influence of interfacial interactions on the conductivity and phase behaviour of organic ionic plastic crystal/polymer nanoparticle composite electrolytes. *J. Mater. Chem. A* **2020**, *8*, 5350–5362. [[CrossRef](#)]
33. Yang, K.; Zhang, Z.; Liao, Z.; Yang, L.; Hirano, S. Organic ionic plastic crystal-polymer solid electrolytes with high ionic conductivity and mechanical ability for solid-state lithium-ion batteries. *Chem. Sel.* **2018**, *3*, 12595–12599. [[CrossRef](#)]
34. Sun, Y.; Jin, F.; Li, J.; Liu, B.; Chen, X.; Dong, H.; Mao, Y.; Gu, W.; Xu, J.; Shen, Y.; et al. Composite solid electrolyte for solid-state lithium batteries workable at room temperature. *ACS Appl. Energy Mater.* **2020**, *3*, 12127–12133. [[CrossRef](#)]
35. Zha, W.; Li, J.; Li, W.; Sun, C.; Wen, Z. Anchoring succinonitrile by solvent-Li<sup>+</sup> associations for high-performance solid-state lithium battery. *Chem. Eng. J.* **2021**, *406*, 126754. [[CrossRef](#)]
36. Xue, C.; Zhang, X.; Wang, S.; Li, L.; Nan, C.W. Organic-organic composite electrolyte enables ultralong cycle life in solid-state lithium metal batteries. *ACS Appl. Mater. Interfaces* **2020**, *12*, 24837–24844. [[CrossRef](#)] [[PubMed](#)]
37. Zhang, X.; Wang, S.; Xue, C.; Xin, C.; Lin, Y.; Shen, Y.; Li, L.; Nan, C.W. Self-suppression of lithium dendrite in all-solid-state lithium metal batteries with poly(vinylidene difluoride)-based solid electrolytes. *Adv. Mater.* **2019**, *31*, 1806082. [[CrossRef](#)]
38. Shen, Z.; Zhong, J.; Xie, W.; Chen, J.; Ke, X.; Ma, J.; Shi, Z. Effect of LiTFSI and LiFSI on cycling performance of lithium metal batteries using thermoplastic polyurethane/halloysite nanotubes solid electrolyte. *Acta Metall. Sin.* **2021**, *34*, 359–372. [[CrossRef](#)]
39. Kuai, Y.; Wang, F.; Yang, J.; Lu, H.; Xu, Z.; Xu, X.; NuLi, Y.; Wang, J. Silica-nanoresin crosslinked composite polymer electrolyte for ambient-temperature all-solid-state lithium batteries. *Mater. Chem. Front.* **2021**, *5*, 6502–6511. [[CrossRef](#)]
40. Wang, X.; Chen, F.; Girard, G.M.A.; Zhu, H.; MacFarlane, D.R.; Mecerreyes, D.; Armand, M.; Howlett, P.C.; Forsyth, M. Poly(ionic liquid)s-in-salt electrolytes with co-coordination-assisted lithium-ion transport for safe batteries. *Joule* **2019**, *3*, 2687–2702. [[CrossRef](#)]
41. Zhang, H.; Feng, W.; Zhou, Z.; Nie, J. Composite electrolytes of lithium salt/polymeric ionic liquid with bis(fluorosulfonyl)imide. *Solid State Ion.* **2014**, *256*, 61–67. [[CrossRef](#)]
42. Kimura, K.; Yajima, M.; Tominaga, Y. A highly-concentrated poly(ethylene carbonate)-based electrolyte for all-solid-state Li battery working at room temperature. *Electrochem. Commun.* **2016**, *66*, 46–48. [[CrossRef](#)]
43. Kimura, K.; Tominaga, Y. Understanding electrochemical stability and lithium ion-dominant transport in concentrated poly(ethylene carbonate) electrolyte. *ChemElectroChem* **2018**, *5*, 4008–4014. [[CrossRef](#)]
44. Tominaga, Y.; Yamazaki, K. Fast Li-ion conduction in poly(ethylene carbonate)-based electrolytes and composites filled with TiO<sub>2</sub> nanoparticles. *Chem. Commun.* **2014**, *50*, 4448–4450. [[CrossRef](#)] [[PubMed](#)]
45. Judez, X.; Zhang, H.; Li, C.; Gonzalez-Marcos, J.A.; Zhou, Z.; Armand, M.; Rodríguez-Martínez, L.M. Lithium bis(fluorosulfonyl)imide/poly(ethylene oxide) polymer electrolyte for all solid-state Li-S cell. *J. Phys. Chem. Lett.* **2017**, *8*, 1956–1960. [[CrossRef](#)] [[PubMed](#)]
46. Eshetu, G.G.; Judez, X.; Li, C.; Martínez-Ibañez, M.; Gracia, I.; Bondarchuk, O.; Carrasco, J.; Rodríguez-Martínez, L.M.; Zhang, H.; Armand, M. Ultrahigh performance all solid-state lithium sulfur batteries: Salt anion's chemistry-induced anomalous synergistic effect. *J. Am. Chem. Soc.* **2018**, *140*, 9921–9933. [[CrossRef](#)]
47. Judez, X.; Zhang, H.; Li, C.; Eshetu, G.G.; Zhang, Y.; Gonzalez-Marcos, J.A.; Armand, M.; Rodríguez-Martínez, L.M. Polymer-rich composite electrolytes for all-solid-state Li-S cells. *J. Phys. Chem. Lett.* **2017**, *8*, 3473–3477. [[CrossRef](#)]
48. Eshetu, G.G.; Judez, X.; Li, C.; Bondarchuk, O.; Rodríguez-Martínez, L.M.; Zhang, H.; Armand, M. Lithium azide as an electrolyte additive for all-solid-state lithium-sulfur batteries. *Angew. Chem. Int. Ed.* **2017**, *56*, 15368–15372. [[CrossRef](#)] [[PubMed](#)]
49. Aldalur, I.; Armand, M.; Zhang, H. Jeffamine-based polymers for rechargeable batteries. *Batter. Supercaps* **2019**, *3*, 30–46. [[CrossRef](#)]
50. Song, Z.; Wang, X.; Wu, H.; Feng, W.; Nie, J.; Yu, H.; Huang, X.; Armand, M.; Zhang, H.; Zhou, Z. Bis(fluorosulfonyl)imide-based electrolyte for rechargeable lithium batteries: A perspective. *J. Power Sources Adv.* **2022**, *14*, 100088. [[CrossRef](#)]
51. Lopez-Aranguren, P.; Judez, X.; Chakir, M.; Armand, M.; Buannic, L. High voltage solid state batteries: Targeting high energy density with polymer composite electrolytes. *J. Electrochem. Soc.* **2020**, *167*, 020548. [[CrossRef](#)]
52. Orue, A.; Arrese-Igor, M.; Cid, X.; Judez, X.; Gomez, N.; López del Amo, J.M.; Manalastas, W.; Srinivasan, M.; Rojviriyaa, C.; Armand, M.; et al. Enhancing the polymer electrolyte–Li metal interface on high-voltage solid-state batteries with Li-based additives inspired by the surface chemistry of Li<sub>7</sub>La<sub>3</sub>Zr<sub>2</sub>O<sub>12</sub>. *J. Mater. Chem. A* **2022**, *10*, 2352–2361. [[CrossRef](#)]

53. Deng, P.L.; Zhang, H.; Feng, W.; Zhou, Z.; Armand, M.; Nie, J. Lithium (fluorosulfonyl) (pentafluoroethylsulfonyl)imide/poly(ethylene oxide) polymer electrolyte: Physical and electrochemical properties. *Solid State Ion.* **2019**, *338*, 161–167. [[CrossRef](#)]
54. Martinez-Ibanez, M.; Sannchez-Diez, E.; Oteo, U.; Gracia, I.; Aldalur, I.; Eitouni, H.B.; Joost, M.; Armand, M.; Zhang, H. Anions with a dipole: Toward high transport numbers in solid polymer electrolytes. *Chem. Mater.* **2022**, *34*, 3451–3460. [[CrossRef](#)]
55. Bouchet, R.; Maria, S.; Meziane, R.; Aboulaich, A.; Liénafa, L.; Bonnet, J.-P.; Phan, T.; Bertin, D.; Gibmes, D.; Devaux, D.; et al. Single-ion BAB triblock copolymers as highly efficient electrolytes for lithium-metal batteries. *Nat. Mater.* **2013**, *12*, 452–457. [[CrossRef](#)]
56. Meabe, L.; Lago, N.; Rubatat, L.; Li, C.; Müller, A.J.; Sardon, H.; Armand, M.; Mecerreyes, D. Polycondensation as a versatile synthetic route to aliphatic polycarbonates for solid polymer electrolytes. *Electrochim. Acta* **2017**, *237*, 259–266. [[CrossRef](#)]
57. Meabe, L.; Huynh, T.V.; Mantione, D.; Porcarelli, L.; Li, C.; O'Dell, L.A.; Sardon, H.; Armand, M.; Forsyth, M.; Mecerreyes, D. UV-cross-linked poly(ethylene oxide carbonate) as free standing solid polymer electrolyte for lithium batteries. *Electrochim. Acta* **2019**, *302*, 414–421. [[CrossRef](#)]
58. Arrese-Igor, M.; Martinez-Ibanez, M.; del Amo, J.M.L.; Sanchez-Diez, E.; Shanmukaraj, D.; Dumond, E.; Armand, M.; Aguesse, F.; Lopez-Aranguren, P. Enabling double layer polymer electrolyte batteries: Overcoming the Li-salt interdiffusion. *Energy Storage Mater.* **2022**, *45*, 578–585. [[CrossRef](#)]
59. Arrese-Igor, M.; Martinez-Ibanez, M.; Pavlenko, E.; Forsyth, M.; Zhu, H.; Armand, M.; Aguesse, F.; Lopez-Aranguren, P. Toward high-voltage solid-state Li-metal batteries with double-layer polymer electrolytes. *ACS Energy Lett.* **2022**, *7*, 1473–1480. [[CrossRef](#)]
60. Martinez-Ibanez, M.; Sanchez-Diez, E.; Qiao, L.X.; Zhang, Y.; Judez, X.; Santiago, A.; Aldalur, I.; Carrasco, J.; Zhu, H.J.; Forsyth, M.; et al. Unprecedented improvement of single Li-ion conductive solid polymer electrolyte through salt additive. *Adv. Funct. Mater.* **2020**, *30*, 2000455. [[CrossRef](#)]
61. Hao, S.-M.; Liang, S.; Sewell, C.D.; Li, Z.; Zhu, C.; Xu, J.; Lin, Z. Lithium-conducting branched polymers: New paradigm of solid-state electrolytes for batteries. *Nano Lett.* **2021**, *21*, 7435–7447. [[CrossRef](#)]
62. Shi, H.F.; Zhao, Y.; Dong, X.; Zhou, Y.; Wang, D.J. Frustrated crystallization and hierarchical self-assembly behaviour of comb-like polymers. *Chem. Soc. Rev.* **2013**, *42*, 2075–2099. [[CrossRef](#)] [[PubMed](#)]
63. Zhang, X.; Daigle, J.C.; Zaghbi, K. Comprehensive review of polymer architecture for all-solid-state lithium rechargeable batteries. *Materials* **2020**, *13*, 2488. [[CrossRef](#)] [[PubMed](#)]
64. Wang, X.; Song, Z.; Wu, H.; Nie, J.; Feng, W.; Yu, H.; Huang, X.; Armand, M.; Zhou, Z.; Zhang, H. Unprecedented impact of main chain on comb polymer electrolytes performances. *ChemElectroChem* **2022**, *9*, 202101590. [[CrossRef](#)]
65. Kasnatscheew, J.; Rodehorst, U.; Streipert, B.; Wiemers-Meyer, S.; Jakelski, R.; Wagner, R.; Laskovic, I.C.; Winter, M. Learning from overpotentials in lithium-ion batteries: A case study on the  $\text{LiNi}_{1/3}\text{Co}_{1/3}\text{Mn}_{1/3}\text{O}_2$  (NCM) cathode. *J. Electrochem. Soc.* **2016**, *163*, A2943–A2950. [[CrossRef](#)]
66. Li, Y.; Lu, Y.; Adelhelm, P.; Titirici, M.-M.; Hu, Y.-S. Intercalation chemistry of graphite: Alkali metal ions and beyond. *Chem. Soc. Rev.* **2019**, *48*, 465–4687. [[CrossRef](#)] [[PubMed](#)]
67. Grillet, A.C.; Humplik, T.; Stirrup, E.K.; Roberts, S.A.; Barringer, D.A.; Snyder, C.M.; Janvrin, M.R.; Apblett, C.A. Conductivity degradation of polyvinylidene fluoride composite binder during cycling: Measurements and simulations for lithium-ion batteries. *J. Electrochem. Soc.* **2016**, *163*, A1859–A1871. [[CrossRef](#)]
68. Cholewinski, A.; Si, P.; Uceda, M.; Pope, M.; Zhao, B. Polymer binders: Characterization and development toward aqueous electrode fabrication for sustainability. *Polymers* **2021**, *13*, 631. [[CrossRef](#)]
69. Wang, Y.-B.; Yang, Q.; Guo, X.; Yang, S.; Chen, A.; Liang, G.-J.; Zhi, C.-Y. Strategies of binder design for high-performance lithium-ion batteries: A mini review. *Rare Met.* **2022**, *41*, 745–761. [[CrossRef](#)]
70. Li, S.; Lorandi, F.; Wang, H.; Liu, T.; Whitacre, J.F.; Matyjaszewski, K. Functional polymers for lithium metal batteries. *Prog. Polym. Sci.* **2021**, *122*, 101453. [[CrossRef](#)]
71. Li, J.; Fleetwood, J.; Hawley, W.B.; Kays, W. From materials to cell: State-of-the-art and prospective technologies for lithium-ion battery electrode processing. *Chem. Rev.* **2022**, *122*, 903–956. [[CrossRef](#)]
72. Pieczonka, N.P.W.; Borgel, V.; Ziv, B.; Leifer, N.; Dargel, V.; Aurbach, D.; Kim, J.-H.; Liu, Z.; Huang, X.; Krachkovskiy, S.A.; et al. Lithium polyacrylate (LiPAA) as an advanced binder and a passivating agent for high-voltage Li-ion batteries. *Adv. Energy Mater.* **2015**, *5*, 1501008. [[CrossRef](#)]
73. Kim, N.-Y.; Moon, J.; Ryou, M.-H.; Kim, S.-H.; Kim, J.-H.; Kim, J.-M.; Bang, J.; Lee, S.-Y. Amphiphilic bottlebrush polymeric binders for high-mass-loading cathodes in lithium-ion batteries. *Adv. Energy Mater.* **2022**, *12*, 2102109. [[CrossRef](#)]
74. Santiago, A.; Sanchez-Diez, E.; Oteo, U.; Aldalur, I.; Echeverria, M.; Armand, M.; Martinez-Ibanez, M.; Zhang, H. Single lithium ion conducting “binderlyte” for high-performing lithium metal batteries. *Small* **2022**, *18*, 2202027. [[CrossRef](#)] [[PubMed](#)]
75. Ott, J.; Völker, B.; Gan, Y.; McMeeking, R.M.; Kamlah, M. A micromechanical model for effective conductivity in granular electrode structures. *Acta Mech. Sin.* **2013**, *29*, 682–698. [[CrossRef](#)]